A complete analytical solution for axial pipeline walking considering seabed resistance as rigid plastic behaviour

YINGHUI TIAN*, WANCHAO WU†, MARK J. CASSIDY* and MARK F. RANDOLPH‡

Offshore pipelines are important infrastructure for transporting oil and gas. They are subjected to cycles of high temperature and pressure variation during operation and shutdown periods, and are therefore susceptible to the stability problem of axial walking due to the asymmetry between the expansion and contraction. Axial walking can cause damage to subsea pipeline systems, for instance to the connected manifolds and steel catenary risers. This paper provides a complete analytical solution to examine the process of pipeline walking based on underlying principles of mechanics, considering the pipeline–seabed sliding response as rigid plastic. The analytical solution allows calculation of the cumulative displacement, strain, axial force and soil resistance along the pipeline under arbitrary temperature or internal pressure change histories, accounting for the coupled contributions from seabed slopes and end tension forces. A dimensionless parameter η is proposed to explain the triggering mechanism for walking by comparing the activating force to the soil resistance. New criteria are established to judge whether pipeline axial walking is possible. Calculation examples are presented in the final part of this paper to demonstrate the analytical solution. This study can be used as a rigorous benchmark and a simple practical tool to evaluate pipeline walking under arbitrary loading histories of temperature and internal pressure variations.

KEYWORDS: offshore engineering; pipes & pipelines; plasticity

INTRODUCTION

Offshore pipelines connect field wells, platforms and onshore processing facilities and are critical infrastructure in the transportation of oil and gas. With developments moving into deeper waters and farther away from coastlines, longer pipelines laid directly on the seabed are required and represent significant capital investment (e.g. export pipelines on the Noth-West Shelf of Australia normally cost more than US$3 million per km (Randolph & Gourvenec, 2011)). To design and protect this investment, research has concentrated on the on-bottom stability and structural integrity of pipelines subjected to hydrodynamic and environmental dynamic loads (examples, among many others, include: Tian & Cassidy, 2008; Tørnes *et al*., 2009; Zeitoun *et al*., 2009; Yu & Yuan, 2014; Draper *et al*., 2015; Tian *et al*., 2015a, 2015b; Yu *et al*., 2017, 2018).

One of the major challenges for deep-water offshore pipelines is the change in high-pressure/high-temperature (HPHT) conditions associated with frequent start-ups and shut-downs during the operational life of the pipe. For instance, the oil production pipelines located in Espírito Santo Basin operate with an inlet temperature of 90°C and internal pressure of 35 MPa (Carneiro *et al*., 2009). The axial strain caused by the HPHT and the asymmetries in the start-up (increasing temperature and pressure) and shut-down (reverting back down to ambient conditions) can cause axial displacements to accumulate over operational cycles, in a ratcheting process, terminologically known as 'pipeline walking' (Tørnes *et al*., 2000; Carr *et al*., 2003). Pipeline walking itself is not the limit state, but can threaten pipeline integrity by causing overstressing at the mid-line for the pipeline or failure at the end connections (Bruton *et al*., 2010; Bruton & Carr, 2011).

Bruton *et al.* (2010) discussed four triggering factors that can cause pipeline walking: (*a*) sustained tension at the ends of a pipeline – for example, pulling forces due to the connections to a steel catenary riser; (*b*) seabed slopes; (*c*) thermal transients; and (*d*) multiphase flow. Carr *et al.* (2006) and Bruton *et al.* (2010) proposed closed-form equations to calculate the walking rate (overall pipeline axial displacement per HPHT cycle) for these scenarios, which are widely adopted for pipeline walking design. However, the solution of Carr *et al.* (2006) and Bruton *et al.* (2010) treated the triggering mechanisms separately, with coupling not considered (Rong *et al*., 2009; Reda *et al*., 2018). There has been an assumption that by simply using superposition, 'conservatism' in design can be maintained (Collberg *et al*., 2011). However, as the results of this paper will highlight, neglecting coupling may significantly underestimate the pipeline walking rate. A pipeline deemed as stable by Carr *et al.* (2006) can still present the possibility of walking. Further, Carr *et al.* (2006) and Bruton *et al.* (2010) only provided equations to calculate the overall walking rate. They did not indicate how to calculate the actual state of the entire pipeline (e.g. displacement, strain, axial force and soil resistance) at any time during the heating and cooling cycles. The ability to predict the state of the pipeline in 'real-time', especially the displacement at the ends, is critical to assess the integrity of pipelines and connected subsea systems. Although recently published numerical studies describe the displacement history for whole HPHT cycles (Castelo *et al*., 2019; Guha *et al*., 2019), a more rigorous and theoretically sound analytical approach is needed to quantify pipeline walking mathematically.

Manuscript received 28 April 2020; revised manuscript accepted 10 February 2021.
Discussion on this paper is welcomed by the editor.
* Department of Infrastructure Engineering, Faculty of Engineering and Information Technology, The University of Melbourne, Victoria, Australia.
† State Key Laboratory of Hydraulic Engineering Simulation and Safety, Tianjin University, Tianjin, P. R. China.
‡ Centre for Offshore Foundation Systems and Ocean Graduate School, The University of Western Australia, Crawley WA, Australia.

This paper presents a complete analytical solution for the process of triggering and development of pipeline walking based on fundamental mechanics, simplifying the pipeline–seabed axial interaction as rigid plastic behaviour. Two factors, seabed slope and tension, are considered, since the two factors essentially have the same driving mechanism, although, as will be demonstrated later, they exhibit coupling effects. To describe the coupled effect between these two factors, a unified parameter (termed the 'activating force' Q) is proposed to account for the combined contribution from the seabed slope and end tension force. A dimensionless parameter η is proposed to explain the ultimate walking triggering mechanism by comparing the activating force to the resistance. The analytical solution addresses the complete pipeline behaviour during axial walking under arbitrary heat-up and cool-down cycles. New criteria – namely, critical pipeline length or equivalent critical mobilising temperature – are established to assess whether a pipeline has the possibility of walking, distinguishing between 'short' and 'long' pipelines – named terminologically after Tørnes *et al.* (2000).

In the following sections, the analytical solution is first presented, starting from the governing equations, and then calculation examples are considered. The aim of this paper is to provide a rigorous and easy-to-use tool for pipeline walking analysis.

GOVERNING EQUATIONS

This section presents the governing equations to prepare for the derivation of the analytical solution. For a thin-walled structure, such as an offshore pipeline, with diameter D and thickness t, internal pressure p causes a hoop stress $\sigma_h = pD/2t$ and a longitudinal stress $\sigma_l = pD/4t$. This will lead to axial strain $\varepsilon = (0{\cdot}5 - \nu)pD/2Et$, where E is the Young's modulus and ν is the Poisson's ratio. A change in pipeline temperature ΔT can cause axial strain $\varepsilon = \alpha\Delta T$, where α is the coefficient of linear expansion. For simplicity in the following equation derivation, the internal pressure change Δp can be expressed as an equivalent temperature change ΔT (see Palmer & Baldry, 1974; Hobbs, 1984; Zhou *et al.*, 2019)

$$\Delta p = \frac{2E}{0{\cdot}5 - \nu}\frac{t}{D}\alpha\Delta T \tag{1}$$

Hereafter, for simplicity, only temperature is used to derive the analytical solution, while the pipe internal pressure can easily be accounted for in an equivalent manner by using equation (1).

Coordinate system and symbol convention

As shown in Fig. 1, the pipeline is considered to be resting on a seabed with a slope angle of θ, and with tensional loads applied at both ends. The tension at the upper end (left-hand end in Fig. 1) of the pipeline is denoted as F_t, and the tension at the bottom end is denoted as F_b. The coordinate system origin is located at the initial position of the left end of the pipeline with the positive x direction being downslope along the pipeline.

Pipe–soil interaction

The pipeline–seabed sliding response is considered as rigid plastic, noting that this is a simplification of the real pipe–soil interaction (see Bruton *et al.*, 2006, 2008, 2009, 2015; Hill & Jacob, 2008; White *et al.*, 2011, 2015; Low *et al.*, 2017 for more details about pipe–soil interaction). As shown in Fig. 2, if the pipeline segment exhibits a tendency to move along the x-axis, the soil resistance is defined as positive, and if the pipeline segment tends to move in the negative direction on the x-axis, the soil resistance is defined as negative. The pipeline weight w per unit length is considered as uniform in this study, and thus the soil axial resistance $f(x)$ at a point of coordinate x can be given as

$$f(x) = \begin{cases} \mu w\cos\theta & \Delta u > 0 \\ f_0 & \Delta u = 0 \\ -\mu w\cos\theta & \Delta u < 0 \end{cases} \tag{2}$$

where μ is the coefficient of friction; f_0 is the soil resistance in the previous step; and Δu represents the increment in motion of the pipeline segment, defined as positive if the pipeline segment tends to move along the x-axis in a positive direction.

Equilibrium of the pipeline

Axial pipeline forces $N(x)$, a function of the coordinate x, are induced due to soil resistance $f(x)$, the tensile forces F_t and F_b and the pipeline weight component $w\sin\theta$. The

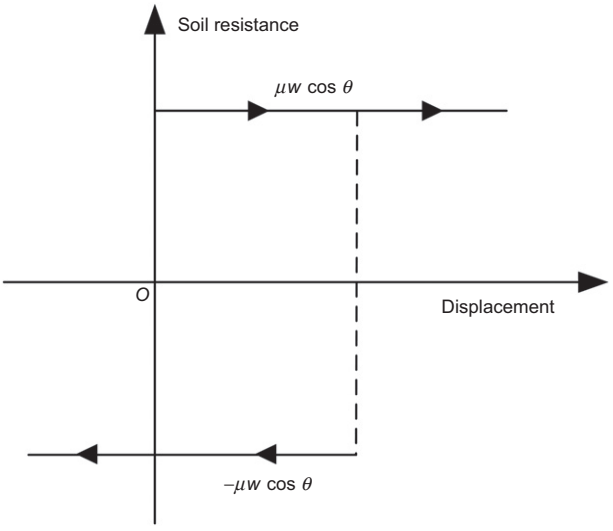

Fig. 2. Rigid plastic model for soil resistance

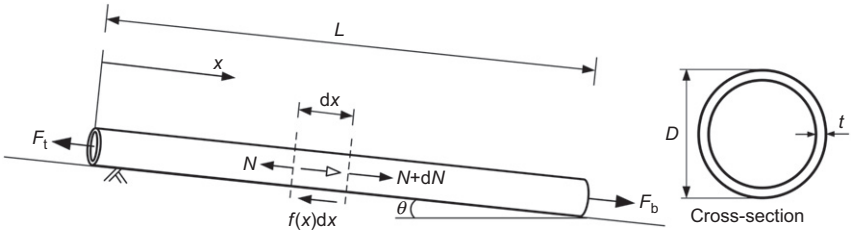

Fig. 1. Pipeline calculation model and sign convention

equilibrium condition for an infinitesimal segment of pipeline shown in Fig. 1 gives

$$N(x) + f(x)\mathrm{d}x = N(x) + \mathrm{d}N(x) + w\ \sin\theta \mathrm{d}x \tag{3}$$

$$\frac{\mathrm{d}N(x)}{\mathrm{d}x} = f\,(x) - w\sin\theta \tag{4}$$

where $N(0) = F_\mathrm{t}$ and $N(L) = F_\mathrm{b}$. Upon integrating equation (4), the axial force $N(x)$ along the pipeline satisfies

$$\begin{aligned} N(x) &= \int_0^x [f(x) - w\sin\theta]\mathrm{d}x + F_\mathrm{t} \\ &= \int_L^x [f(x) - w\sin\theta]\mathrm{d}x + F_\mathrm{b} \end{aligned} \tag{5}$$

where L is the pipeline length. A positive value of N indicates tensile axial force and a negative value indicates compression.

The strain along the pipeline $\varepsilon(x)$ can be written as

$$\varepsilon(x) = \alpha T + \frac{N(x)}{EA} \tag{6}$$

where α is the coefficient of linear expansion of the pipeline; T is the temperature change relative to the initial state; E is the Young's modulus of the pipeline material; and A is the cross-sectional area of the pipeline, giving axial rigidity EA.

In the process of heating-up and cooling-down cycles, pipelines tend to expand and contract. The pipeline displacement $u(x)$ can then be expressed as

$$u(x) = \int_{x_S}^x \varepsilon(x)\mathrm{d}x + u_S \tag{7}$$

where u_S is the displacement of an arbitrarily selected point S at coordinate x_S. For a specific heating or cooling process, a stationary point exists, referred to as a 'virtual anchor' (Carr *et al.*, 2006). It is convenient to take point S as the virtual anchor point because it does not move during the particular heating or cooling process.

As the boundary condition of a quasi-static problem, the soil resistance $f(x)$ along the pipeline always balances the external force, so that

$$\begin{aligned} \int_0^L f\,(x)\mathrm{d}x &= wL\sin\theta + F_\mathrm{b} - F_\mathrm{t} \\ &= W\sin\theta + F_\mathrm{b} - F_\mathrm{t} = Q \end{aligned} \tag{8}$$

where $W = wL$ is the total pipeline weight. $Q = W\sin\theta + F_\mathrm{b} - F_\mathrm{t}$ is termed the 'activating force' in this paper, combining the two contributions of $W\sin\theta$ and resultant tension force $F = F_\mathrm{b} - F_\mathrm{t}$.

As demonstrated later, Q is the underlying reason for axial walking, with no axial walking occurring if $Q = 0$. In essence, the seabed slope and tension both contribute to Q with a similar driving mechanism. This is the reason why this paper considers the two triggering factors of seabed slope and end tension force, while the other two triggering factors (i.e. thermal transients and multiphase flow, as discussed by Bruton *et al.* (2010)) have different mechanisms and are not considered here.

In summary, the soil resistance $f(x)$, the axial force $N(x)$, the axial strain $\varepsilon(x)$ and the displacement $u(x)$ along the pipeline are functions of the coordinate x. Owing to the assumed rigid plastic model of seabed resistance, the soil resistance $f(x)$ is piecewise constant. The axial force $N(x)$ and strain $\varepsilon(x)$ are piecewise linear functions of the coordinate x and thus the displacement $u(x)$ shows a quadratic variation with x. These constitute a simultaneous equation system, the solution of which is examined in the following section.

PIPELINE BEHAVIOUR DURING HEATING UP AND COOLING DOWN

This section solves the equation system of equations (5)–(7) for cycles of heating up and cooling down with arbitrary amplitudes. As indicated in Fig. 3

(*a*) T_ini is the initial temperature of the pipeline
(*b*) $T_{\mathrm{H},1}$, $T_{\mathrm{H},2}$ and $T_{\mathrm{H},3}$ denote the peak temperatures (i.e. at the ends of heating cycles) in the first, second and third cycles, respectively
(*c*) $T_{\mathrm{C},1}$, $T_{\mathrm{C},2}$ and $T_{\mathrm{C},3}$ are the trough temperatures (i.e. at the ends of cooling cycles) in the first, second and third cycles, respectively;
(*d*) δT_h of the nth cycle denotes the increase in temperature during the heating process relative to the previous cycle temperature trough $T_{\mathrm{C},n-1}$
(*e*) δT_c of the nth cycle is the amplitude (i.e. positive) of the temperature reduction during the cooling process relative to the current peak temperature $T_{\mathrm{H},n}$
(*f*) ΔT represents the real-time temperature difference relative to the initial temperature T_ini.

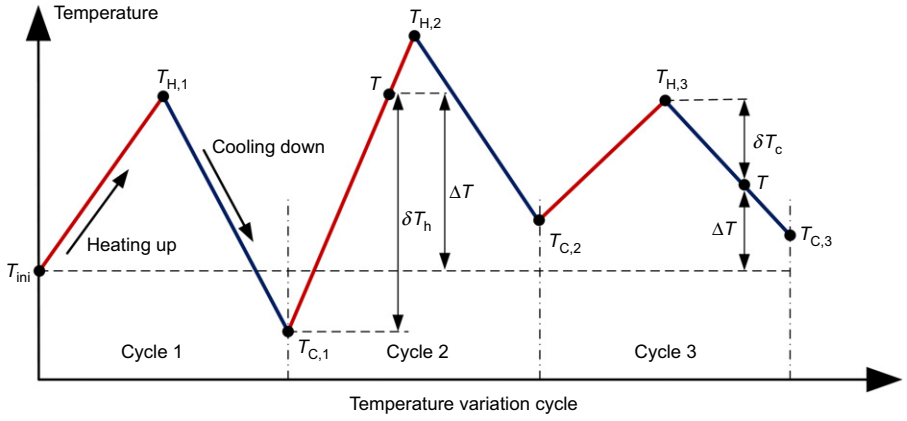

Fig. 3. Temperature variation

As noted, the notation convention here is to use δ to denote the relative temperature change compared to the previous peak or trough and Δ to denote the temperature difference compared to the initial temperature T_{ini}.

Initial state

It is assumed that the initial state corresponds to a pipeline sitting on a sloped seabed prior to the application of tension F_t and F_b, with initial displacement, strain and axial force all zero, that is, $u(x) = 0$, $\varepsilon(x) = 0$ and $N(x) = 0$. With the rigid plastic model adopted for the seabed resistance, this is consistent with taking the soil resistance $f(x)$ of the pipeline as $w\sin\theta$ (although this is a somewhat arbitrary choice, given the redundancy of the rigid plastic model).

When tensile forces F_t and F_b are applied, pipeline deformation occurs. The length of the deformed region at the left side under tension F_t is denoted as X_L and the length of the deformed region at the right side under tension F_b is denoted as X_R. The soil resistance distribution $f(x)$ is as shown in Fig. 4(a), while the axial force $N(x)$ and the strain $\varepsilon(x)$ and the displacement $u(x)$ are shown in Figs 4(b)–4(d), for conditions after applying tension forces F_t, F_b but with $\Delta T = 0$. It is noted that the strain $\varepsilon(x)$ and displacement $u(x)$ within the X_L and X_R regions vary linearly and quadratically with x. The slopes of the axial force lines in Fig. 4(b) are $-(\mu\cos\theta + w\sin\theta)w$ and $(\mu\cos\theta - \sin\theta)w$ at the left and right ends of the pipeline, respectively. Noting $\mu w\cos\theta$ is the friction resistance and $w\sin\theta$ is the sliding component of pipeline weight, the positive and negative sign reflect the balance between these two items.

Considering the boundary conditions of F_t, F_b and $\varepsilon(x) = 0$ within the central segment of $[X_L,\ L - X_R]$, the length of X_L and X_R can be calculated from equations (5) and (6) as

$$\begin{cases} \dfrac{X_L}{L} = \dfrac{F_t}{W}\dfrac{1}{\mu\cos\theta + \sin\theta} \\ \dfrac{X_R}{L} = \dfrac{F_b}{W}\dfrac{1}{\mu\cos\theta - \sin\theta} \end{cases} \tag{9}$$

First heating-up process

The first heating-up process is a special situation because the seabed soil resistance to the pipeline in the initial state is yet to be fully mobilised, whereas the subsequent cooling-down and re-heating-up cycles start from a fully mobilised state.

At the start of the first heating cycle, before fully mobilising the soil resistance along the pipeline, the lengths X_L and X_R of the end sections of the fully mobilised sliding resistance increase. The soil resistance $f(x)$ of the 'stationary segment' $[X_L,\ L - X_R]$ is maintained as $w\sin\theta$ (Fig. 4(a)), corresponding to the status of 'before full mobilisation'.

$$f(x) = \begin{cases} -\mu w\cos\theta & x \in [0, X_L] \\ w\sin\theta & x \in [X_L, L - X_R] \\ \mu w\cos\theta & x \in [L - X_R, L] \end{cases} \tag{10}$$

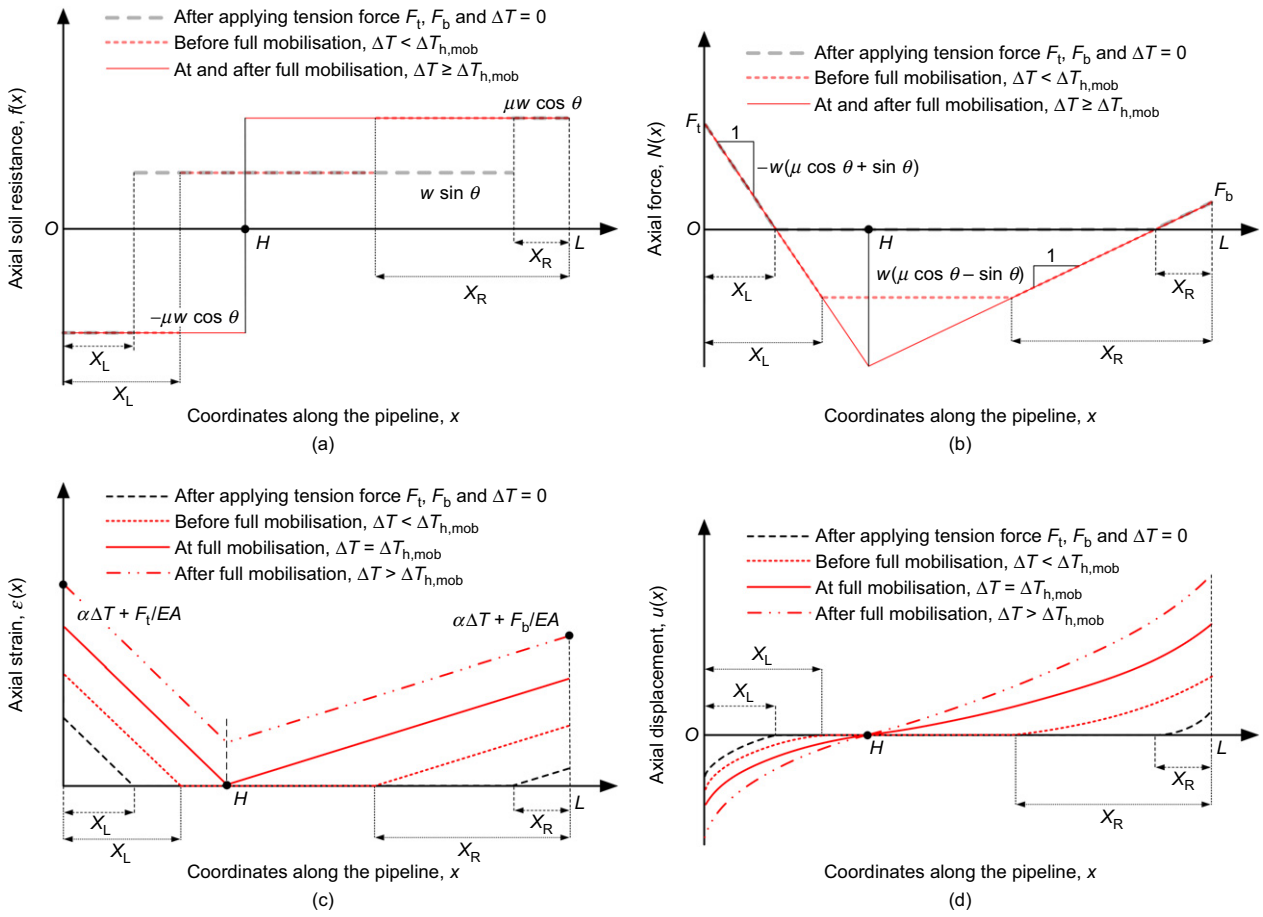

Fig. 4. Pipeline during first heating up period: (a) soil resistance; (b) axial force; (c) axial strain; (d) axial displacement

The axial force $N(x)$ can be integrated from the soil resistance $f(x)$ (Fig. 4(b))

$$N(x) = \begin{cases} -(\mu\cos\theta + \sin\theta)wx + F_t & x \in [0, X_L] \\ -(\mu\cos\theta + \sin\theta)wX_L + F_t = & \\ -(\mu\cos\theta - \sin\theta)w(L - X_R) + F_b & x \in [X_L, L - X_R] \\ -(\mu\cos\theta - \sin\theta)w(L - x) + F_b & x \in [L - X_R, L] \end{cases} \tag{11}$$

Again note that the slopes of axial force are $-(\mu\cos\theta + \sin\theta)w$ and $(\mu\cos\theta - \sin\theta)w$ at the two ends. The axial force at the stationary section is not zero, but as shown in Fig. 4(c) due to the temperature change.

The strain distribution $\varepsilon(x)$ can be calculated from the axial force $N(x)$ using equations (6) and (11) (with a similar pattern as Fig. 4(c)).

$$\varepsilon(x) = \begin{cases} \alpha\Delta T + \dfrac{F_t}{EA} - (\mu\cos\theta + \sin\theta)\dfrac{W}{EA}\dfrac{x}{L} & x \in [0, X_L] \\ \alpha\Delta T + \dfrac{F_t}{EA} - (\mu\cos\theta + \sin\theta)\dfrac{W}{EA}\dfrac{X_L}{L} = 0 & x \in [X_L, L - X_R] \\ \alpha\Delta T + \dfrac{F_b}{EA} - (\mu\cos\theta - \sin\theta)\dfrac{W}{EA}\left(\dfrac{L - x}{L}\right) & x \in [L - X_R, L] \end{cases} \tag{12}$$

Since the middle segment $[X_L, L - X_R]$ of the pipeline is stationary, the strain $\varepsilon(x)$ is 0 and the length of X_L and X_R now becomes

$$\begin{cases} \dfrac{X_L}{L} = \left(\alpha\Delta T\dfrac{EA}{W} + \dfrac{F_t}{W}\right)\dfrac{1}{\mu\cos\theta + \sin\theta} \\ \dfrac{X_R}{L} = \left(\alpha\Delta T\dfrac{EA}{W} + \dfrac{F_b}{W}\right)\dfrac{1}{\mu\cos\theta - \sin\theta} \end{cases} \tag{13}$$

It is obvious from the comparison with equation (9) that the changes of X_L and X_R arise due to the temperature change ΔT.

The displacement $u(x)$ of the pipeline during the first heating process can be calculated based on equation (7), where the point S can be considered as any point in the middle stationary segment $[X_L, L - X_R]$

$$\frac{u(x)}{L} = \begin{cases} -\dfrac{\mu\cos\theta + \sin\theta}{2}\dfrac{W}{EA}\left(\dfrac{x}{L}\right)^2 + \left(\alpha\Delta T + \dfrac{F_t}{EA}\right)\dfrac{x}{L} - \dfrac{1}{2(\mu\cos\theta + \sin\theta)}\dfrac{EA}{W}\left(\alpha\Delta T + \dfrac{F_t}{EA}\right)^2 & x \in [0, X_L] \\ 0 & x \in [X_L, L - X_R] \\ \dfrac{\mu\cos\theta - \sin\theta}{2}\dfrac{W}{EA}\left(\dfrac{L - x}{L}\right)^2 - \left(\alpha\Delta T + \dfrac{F_b}{EA}\right)\dfrac{L - x}{L} + \dfrac{1}{2(\mu\cos\theta - \sin\theta)}\dfrac{EA}{W}\left(\alpha\Delta T + \dfrac{F_b}{EA}\right)^2 & x \in [L - X_R, L] \end{cases} \tag{14}$$

Again, the factors of the second-order terms reflect the balance between the sliding component of self-weight $W\sin\theta$ and soil resistance $\mu W\cos\theta$ (normalised with axial rigidity EA). The factor $(\alpha\Delta T + F_t/EA)$ or $(\alpha\Delta T + F_b/EA)$ of the first-order terms is the strain at either end of the pipeline. The third terms are the displacements of the pipe ends.

With increasing temperature change, the pipeline stationary segment $[X_L, L - X_R]$ reduces and eventually shrinks into a single point denoted as H (i.e. the virtual anchor point during heating up), with the coordinate denoted as x_H. The corresponding temperature increase – that is, the temperature mobilising the full pipeline in the first heating cycle – is denoted as $\Delta T_{h,mob}$, which corresponds to the length of stationary segment $[X_L, L–X_R]$ reduced to 0 – that is, $X_L + X_R = L$. Thus, the stationary point H divides the pipeline into a left and a right segment. The left segment moves in the negative uphill direction and the right segment moves in the positive downhill direction. The full mobilisation of the soil resistance $f(x)$ along the pipeline is as shown in Fig. 4(a).

$$f(x) = \begin{cases} -\mu w\cos\theta & x \in [0, x_H] \\ \mu w\cos\theta & x \in [x_H, L] \end{cases} \tag{15}$$

Consequently, the axial force $N(x)$ and the axial strain $\varepsilon(x)$ distribution of the pipeline are

$$N(x) = \begin{cases} -(\mu\cos\theta + \sin\theta)wx + F_t & x \in [0, x_H] \\ (\mu\cos\theta - \sin\theta)w(x - L) + F_b & x \in [x_H, L] \end{cases} \tag{16}$$

$$\varepsilon(x) = \begin{cases} \alpha\Delta T + \dfrac{F_t}{EA} - (\mu\cos\theta + \sin\theta)\dfrac{W}{EA}\dfrac{x}{L} & x \in [0, x_H] \\ \alpha\Delta T + \dfrac{F_b}{EA} - (\mu\cos\theta - \sin\theta)\dfrac{W}{EA}\left(\dfrac{L - x}{L}\right) & x \in [x_H, L] \end{cases} \tag{17}$$

With equations (5) and (8), the coordinate of point H, x_H, can be calculated

$$\frac{x_H}{L} = \frac{1}{2}\left(1 - \frac{Q}{\mu W\cos\theta}\right) = \frac{1}{2}(1 - \eta) \tag{18}$$

where η is defined as $Q/\mu W\cos\theta$, the ratio of activating force Q to the soil sliding resistance $\mu W\cos\theta$. Obviously, η must fall within the range from -1 to 1; otherwise, the pipeline system could not maintain equilibrium. It can be inferred that the position of H can be either at the left or right side of the pipe midpoint $x_{mid} = L/2$ (with an offset distance of ηL), depending on the direction of Q. Similarly, a virtual anchor

point C appears in the cooling process, as will be discussed later.

The displacement distribution $u(x)$ of the pipeline after full mobilisation during the first heating cycle is as shown in Fig. 4(d). Noting equations (17) and (18), the displacement distribution $u(x)$ can be written as

$$\frac{u(x)}{L}=\begin{cases}-\dfrac{\mu\cos\theta+\sin\theta}{2}\dfrac{W}{EA}\left(\dfrac{x}{L}\right)^2+\left(\alpha\Delta T+\dfrac{F_{\mathrm{t}}}{EA}\right)\dfrac{x}{L}+\left[\dfrac{\mu\cos\theta+\sin\theta}{8}\dfrac{W}{EA}(1-\eta)-\dfrac{1}{2}\left(\alpha\Delta T+\dfrac{F_{\mathrm{t}}}{EA}\right)\right](1-\eta) & x\in[0,x_H]\\ \dfrac{\mu\cos\theta-\sin\theta}{2}\dfrac{W}{EA}\left(\dfrac{L-x}{L}\right)^2-\left(\alpha\Delta T+\dfrac{F_{\mathrm{b}}}{EA}\right)\dfrac{L-x}{L}-\left[\dfrac{\mu\cos\theta-\sin\theta}{8}\dfrac{W}{EA}(1+\eta)-\dfrac{1}{2}\left(\alpha\Delta T+\dfrac{F_{\mathrm{b}}}{EA}\right)\right](1+\eta) & x\in[x_H,L]\end{cases} \tag{19}$$

Comparison with equation (14) shows the first two items are the same. The third terms differ from those in equation (14). This is due to the fact that the strain distribution pattern after full mobilisation differs from that before full mobilisation (see Fig. 4(c)).

Considering equations (13) and (18), the fully mobilised temperature increase $\Delta T_{\mathrm{h,mob}}$ in the first heating up is

$$\Delta T_{\mathrm{h,mob}}=\frac{1}{2\alpha EA}\left[\mu W\cos\theta\left(1-\frac{\tan\theta}{\mu}\eta\right)-(F_{\mathrm{t}}+F_{\mathrm{b}})\right] \tag{20}$$

Cooling down

During a shutdown, the pipeline gradually cools down uniformly and exhibits a tendency to contract. As will be shown later, no walking happens if the preceding maximum temperature is less than the full mobilisation temperature. Herein, cooling down is assumed to follow a preceding fully mobilised heating-up process.

At the start of the nth cooling cycle, the lengths of the regions where the pipeline contracts, relative to the preceding heating-up process, are denoted as X_{S} at the ends of the pipeline (see Fig. 5). These must be equal, because the soil resistance $f(x)$ along the pipeline must satisfy the equilibrium condition of equation (8) during a uniformly cooling process. As shown in Fig. 5(a), the soil resistance at the left end of the pipeline changes from negative to positive, and that at the right end changes from positive to negative. The soil resistance in the middle of the pipeline does not change because the middle part of the pipeline has yet to be re-mobilised. The distribution of the soil resistance $f(x)$ is

$$f(x)=\begin{cases}\mu w\cos\theta & x\in[0,X_{\mathrm{S}}]\\ -\mu w\cos\theta & x\in[X_{\mathrm{S}},x_H]\\ \mu w\cos\theta & x\in[x_H,L-X_{\mathrm{S}}]\\ -\mu w\cos\theta & x\in[L-X_{\mathrm{S}},L]\end{cases} \tag{21}$$

According to equation (5), the axial force distribution $N(x)$ and strain $\varepsilon(x)$ along the pipeline are

$$N(x)=\begin{cases}(\mu\cos\theta-\sin\theta)wx+F_{\mathrm{t}} & x\in[0,X_{\mathrm{S}}]\\ -(\mu\cos\theta+\sin\theta)w(x-X_{\mathrm{S}}) & \\ \quad -2\sin\theta wX_{\mathrm{S}}+F_{\mathrm{t}} & x\in[X_{\mathrm{S}},x_H]\\ -(\mu\cos\theta-\sin\theta)w(L-X_{\mathrm{S}}-x) & \\ \quad +(\mu\cos\theta+\sin\theta)wX_{\mathrm{S}}+F_{\mathrm{b}} & x\in[x_H,L-X_{\mathrm{S}}]\\ (\mu\cos\theta+\sin\theta)w(L-x)+F_{\mathrm{b}} & x\in[L-X_{\mathrm{S}},L]\end{cases} \tag{22}$$

$$\varepsilon(x)=\begin{cases}\alpha\Delta T+\dfrac{F_{\mathrm{t}}}{EA}+(\mu\cos\theta-\sin\theta)\dfrac{W}{EA}\dfrac{x}{L} & x\in[0,X_{\mathrm{S}}]\\ \alpha\Delta T+\dfrac{F_{\mathrm{t}}}{EA}-(\mu\cos\theta+\sin\theta)\dfrac{W}{EA}\dfrac{x-X_{\mathrm{S}}}{L}-2\sin\theta\dfrac{W}{EA}\dfrac{X_{\mathrm{S}}}{L} & x\in[X_{\mathrm{S}},x_H]\\ \alpha\Delta T+\dfrac{F_{\mathrm{b}}}{EA}-(\mu\cos\theta-\sin\theta)\dfrac{W}{EA}\dfrac{L-X_{\mathrm{S}}-x}{L}+(\mu\cos\theta+\sin\theta)\dfrac{W}{EA}\dfrac{X_{\mathrm{S}}}{L} & x\in[x_H,L-X_{\mathrm{S}}]\\ \alpha\Delta T+\dfrac{F_{\mathrm{b}}}{EA}+(\mu\cos\theta+\sin\theta)\dfrac{W}{EA}\dfrac{L-x}{L} & x\in[L-X_{\mathrm{S}},L]\end{cases} \tag{23}$$

At this moment, the displacement of the pipeline can be obtained by integrating equation (23), the expression of which is quite lengthy and thus shown in Appendix 1. The length X_{S} can be obtained by noting that the segment of $[X_{\mathrm{S}}, L-X_{\mathrm{S}}]$ is stationary during the cooling (i.e. the displacement accumulated from previous heating up is kept as unchanged) and thus the resultant strain change is zero. This can be interpreted as the change of axial force compensating the strain change caused by cooling down. As shown in Fig. 5(b), the axial force change at each end of the stationary segment $[X_{\mathrm{S}}, L-X_{\mathrm{S}}]$ denoted as ΔN_{C}, can be calculated by noting the change of soil friction $\Delta f(x)$ – that is, the rate of $N(x)$ changing – is $2\mu w\cos\theta$, so that

$$\Delta N_{\mathrm{C}}=2\mu\cos\theta wX_{\mathrm{S}} \tag{24}$$

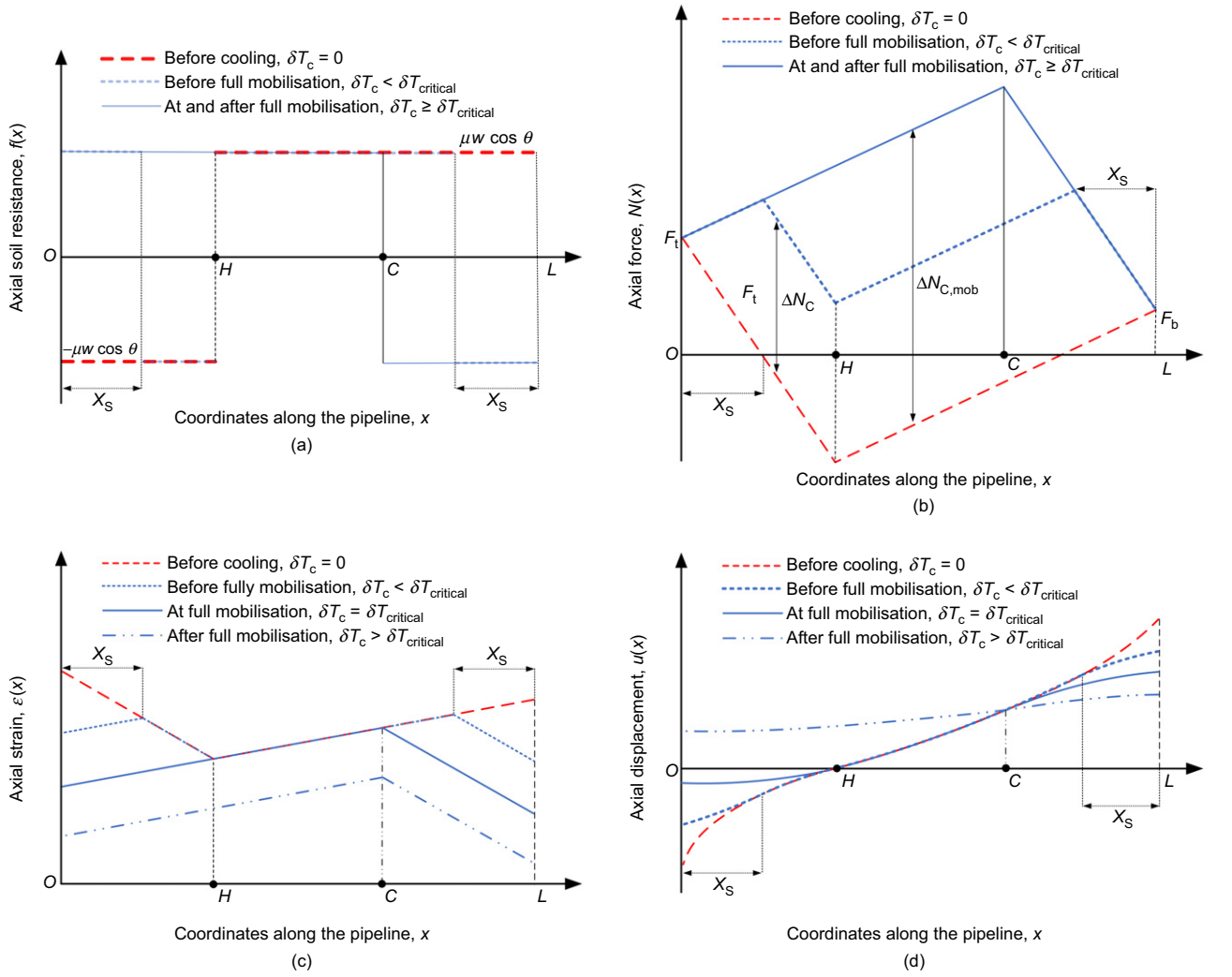

Fig. 5. Pipeline during cooling period: (a) soil resistance; (b) axial force; (c) axial strain; (d) axial displacement

Noting the strain change due to cooling down is $\alpha\delta T_c$, the following relationship holds

$$\alpha\delta T_c = \frac{\Delta N_C}{EA} = 2\mu\cos\theta\frac{W}{EA}\frac{X_S}{L} \tag{25}$$

where the length of the contraction region X_S at each end of the pipeline can be obtained as a relationship of the cooling down temperature increment δT_C

$$\frac{X_S}{L} = \frac{\alpha}{2\mu\cos\theta}\frac{EA}{W}\delta T_c \tag{26}$$

As the pipeline cools further, the length X_S increases and eventually the whole pipeline is mobilised in contraction relative to the preceding heating stage. The corresponding critical cooling-down temperature drop is denoted as $\delta T_{critical}$, where the stationary segment is reduced to one point C with coordinate x_C (see Fig. 5). At this time, the soil resistance distribution $f(x)$ along the pipeline is shown in Fig. 5(a), and is given as

$$f(x) = \begin{cases} \mu w\cos\theta & x \in [0, x_C] \\ -\mu w\cos\theta & x \in [x_C, L] \end{cases} \tag{27}$$

Based on equations (5) and (27), the axial force distribution $N(x)$ can be calculated as

$$N(x) = \begin{cases} (\mu\cos\theta - \sin\theta)wx + F_t & x \in [0, x_C] \\ (\mu\cos\theta + \sin\theta)w(L-x) + F_b & x \in [x_C, L] \end{cases} \tag{28}$$

With equations (6) and (28), the strain distribution $\varepsilon(x)$ along the pipeline is

$$\varepsilon(x) = \begin{cases} \alpha\Delta T + \dfrac{F_t}{EA} + (\mu\cos\theta - \sin\theta)\dfrac{W}{EA}\dfrac{x}{L} & x \in [0, x_C] \\ \alpha\Delta T + \dfrac{F_b}{EA} + (\mu\cos\theta + \sin\theta)\dfrac{W}{EA}\dfrac{L-x}{L} & x \in [x_C, L] \end{cases} \tag{29}$$

Considering equations (8) and (27), point C is located at

$$\frac{x_C}{L} = \frac{1}{2}\left(1 + \frac{Q}{\mu W\cos\theta}\right) = \frac{1}{2}(1+\eta) \tag{30}$$

Again, the position of the C point can be to the left or right of the pipe midpoint, depending on the direction of the activating force, Q.

Combining equations (7) and (29), the displacement distribution $u(x)$ along pipeline during the nth cooling down is

$$\frac{u(x)}{L}=\begin{cases}\dfrac{(\mu\cos\theta-\sin\theta)W}{2EA}\left(\dfrac{x}{L}\right)^2+\left(\alpha\Delta T+\dfrac{F_t}{EA}\right)\dfrac{x}{L}\\ \quad-\left[\dfrac{(\mu\cos\theta-\sin\theta)W}{8EA}(1+\eta)+\dfrac{1}{2}\left(\alpha\Delta T+\dfrac{F_t}{EA}\right)\right](1+\eta)+\dfrac{u_{C,n}}{L} & x\in[0,x_C]\\ -\dfrac{(\mu\cos\theta+\sin\theta)W}{2EA}\left(\dfrac{L-x}{L}\right)^2-\left(\alpha\Delta T+\dfrac{F_b}{EA}\right)\dfrac{L-x}{L}\\ \quad+\left[\dfrac{(\mu\cos\theta+\sin\theta)W}{8EA}(1-\eta)+\dfrac{1}{2}\left(\alpha\Delta T+\dfrac{F_b}{EA}\right)\right](1-\eta)+\dfrac{u_{C,n}}{L} & x\in[x_C,L]\end{cases} \tag{31}$$

where $u_{C,n}$ is the accumulated displacement of the virtual anchor point C in the $n-1$ cycles and the heating process of the nth cycle, noting C is stationary during the cooling down process (Fig. 6).

Noting equations (16) and (28), the value of $\Delta N_{C,mob}$ – that is, the axial force difference between full mobilisation during heating and full re-mobilisation during cooling down is

$$\Delta N_{C,mob}=\mu W\cos\theta-|Q| \tag{32}$$

where the absolute value of Q is due to the fact that stationary points H, C can be at either side of the pipe midpoint depending on the direction (sign) of the activating force, Q. For the case of $Q<0$, the point H is to the right of the midpoint and C is to the left. In this case, the pipe is walking uphill.

The critical temperature drop $\delta T_{critical}$ that mobilises the soil sliding resistance fully during contraction can be calculated from equations (25) and (32) as

$$\delta T_{critical}=\frac{\Delta N_{C,mob}}{\alpha EA}=\frac{\mu W\cos\theta-|Q|}{\alpha EA} \tag{33}$$

Since $\mu W\cos\theta$ is the total soil resistance and Q is the activating force, the numerator $\mu W\cos\theta-|Q|$ reflects the reserve soil resistance. The greater is $\mu W\cos\theta-|Q|$, the greater the temperature change that is required to mobilise the pipeline. The denominator α and EA imply that lower expandability and softer cross-sectional rigidity lead to a greater temperature change to mobilise the pipeline. The difference between equations (20) and (33) is that $\Delta T_{h,mob}$ is relative to T_{ini}, which is only applicable for the first heating process, while $\delta T_{critical}$ is relative to the peak temperature of the nth cycle.

The following heating-up and cooling-down process

When the pipeline is heated up again (the second or subsequent heating up, i.e. any heating process except the first cycle as detailed in the section 'First heating-up process'), the evolution pattern of axial force is similar to the cooling down process just discussed. When the reheating temperature change δT_h is small, the length of the expansion segment at each end of the pipeline can be calculated similarly to equation (26) by using δT_h to substitute δT_c. In fact, except for the first heating, the calculation rules of the heating and cooling process of the pipeline are similar because all those processes are based on a preceding fully mobilised state. Consistently, the critical temperature $\delta T_{critical}$ is the same as in equation (33).

Combining equations (6), (7) and (16), the displacement distribution $u(x)$ of the pipeline during the nth heating up is

$$\frac{u(x)}{L}=\begin{cases}-\dfrac{\mu\cos\theta+\sin\theta}{2}\dfrac{W}{EA}\left(\dfrac{x}{L}\right)^2+\left(\alpha\Delta T+\dfrac{F_t}{EA}\right)\dfrac{x}{L}\\ \quad+\left[\dfrac{\mu\cos\theta+\sin\theta}{8}\dfrac{W}{EA}(1-\eta)-\dfrac{1}{2}\left(\alpha\Delta T+\dfrac{F_t}{EA}\right)\right](1-\eta)+\dfrac{u_{H,n-1}}{L} & x\in[0,x_H]\\ \dfrac{\mu\cos\theta-\sin\theta}{2}\dfrac{W}{EA}\left(\dfrac{L-x}{L}\right)^2-\left(\alpha\Delta T+\dfrac{F_b}{EA}\right)\dfrac{L-x}{L}\\ \quad-\left[\dfrac{\mu\cos\theta-\sin\theta}{8}\dfrac{W}{EA}(1+\eta)-\dfrac{1}{2}\left(\alpha\Delta T+\dfrac{F_b}{EA}\right)\right](1+\eta)+\dfrac{u_{H,n-1}}{L} & x\in[x_H,L]\end{cases} \tag{34}$$

where $u_{H,n-1}$ indicates the accumulated displacement of point H from the previous $n-1$ cycles (see Fig. 6). If the pipeline is in the first heating cycle ($n=1$), equation (14) or equation (19) should be used.

For subsequent cooling, the pipeline behaviour is similar to the first cooling process and thus equations (31) and (45) listed in Appendix 1 can be used again.

WALKING RATE

Incremental walking magnitude

Stationary virtual anchor points, namely, H and C, exist during the heating and cooling processes, with coordinates denoted x_H and x_C, respectively. Fig. 6 illustrates the pipeline displacement pattern subjected to multiple cycles of heating up and cooling down. For a specific nth cycle (except for the first) the displacement of any point of the pipeline can be

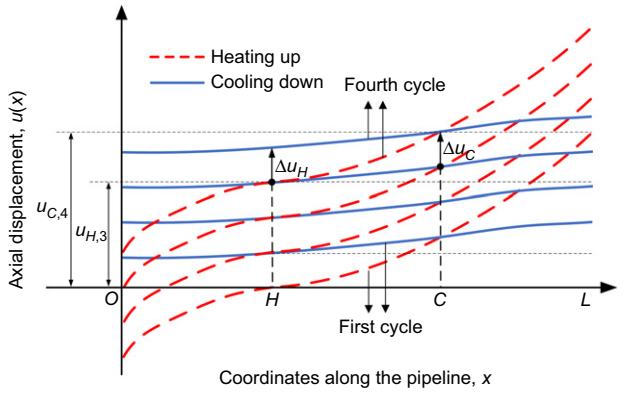

Fig. 6. Illustration of cumulative displacement

evaluated from equations (34) and (31). For the heating up, H is stationary and the displacement of virtual anchor C can be calculated by substituting the coordinate x_C into equation (34), giving

$$\frac{u_{C,n}}{L}-\frac{u_{H,n-1}}{L}=\begin{cases}\left[\alpha\left(T_{\mathrm{c},n-1}+\delta T_{\mathrm{h},n}-T_{\mathrm{ini}}\right)+\dfrac{F_{\mathrm{b}}}{EA}-\dfrac{\mu\cos\theta-\sin\theta}{2}\dfrac{W}{EA}\right]\eta & Q>0\\ \left[\alpha\left(T_{\mathrm{c},n-1}+\delta T_{\mathrm{h},n}-T_{\mathrm{ini}}\right)+\dfrac{F_{\mathrm{t}}}{EA}-\dfrac{\mu\cos\theta+\sin\theta}{2}\dfrac{W}{EA}\right]\eta & Q<0\end{cases} \tag{35}$$

During the following cooling down, point C becomes stationary and the displacement of point H, u_H, can be calculated by substituting the coordinate x_H into equation (31), to give

$$\frac{u_{H,n}}{L}-\frac{u_{C,n}}{L}=\begin{cases}-\left[\alpha\left(T_{\mathrm{c},n-1}+\delta T_{\mathrm{h},n}-\delta T_{\mathrm{c},n}-T_{\mathrm{ini}}\right)+\dfrac{F_{\mathrm{t}}}{EA}+\dfrac{\mu\cos\theta-\sin\theta}{2}\dfrac{W}{EA}\right]\eta & Q>0\\ -\left[\alpha\left(T_{\mathrm{c},n-1}+\delta T_{\mathrm{h},n}-\delta T_{\mathrm{c},n}-T_{\mathrm{ini}}\right)+\dfrac{F_{\mathrm{b}}}{EA}+\dfrac{\mu\cos\theta+\sin\theta}{2}\dfrac{W}{EA}\right]\eta & Q<0\end{cases} \tag{36}$$

The temperature changes $\delta T_{\mathrm{c},n}$ and $\delta T_{\mathrm{h},n}$ are not necessarily the same, implying that the equations can describe the pipe response to arbitrary heating and cooling changes in temperature.

The incremental displacement of point H in the nth cycle can be calculated as $u_{H,n}-u_{H,n-1}$ by combining equation (35) and equation (36) to give

$$\begin{aligned}\frac{\Delta u_H}{L}&=\left(\alpha\delta T-\frac{\mu W\cos\theta-|Q|}{EA}\right)\frac{Q}{\mu W\cos\theta}\\&=\alpha(\delta T-\delta T_{\mathrm{critical}})\eta\end{aligned} \tag{37}$$

where δT is the cooling down temperature change δT_{c}. Similarly, the incremental displacement Δu_C of point C can be calculated from equation (37) by using δT_{h}. Note that δT represents the amplitude of temperature change (thus always positive) compared to the previous peak or trough.

The incremental displacement of the midpoint $\Delta u^{\mathrm{h}}_{\mathrm{mid}}$ during a single heating up ($u_{\mathrm{mid}}-u_{H,n-1}$) or $\Delta u^{\mathrm{c}}_{\mathrm{mid}}$ cooling down ($u_{\mathrm{mid}}-u_{C,n}$) process can be expressed by considering equations (31) and (34), giving

$$\frac{\Delta u^{\mathrm{h,c}}_{\mathrm{mid}}}{L}=\frac{1}{2}\alpha\left(\delta T_{\mathrm{h,c}}-\delta T_{\mathrm{critical}}\right)\eta \tag{38}$$

where δT_{h} or δT_{c} are used, respectively, for heating or cooling to calculate $\Delta u^{\mathrm{h}}_{\mathrm{mid}}$ or $\Delta u^{\mathrm{c}}_{\mathrm{mid}}$.

The midpoint, unlike the virtual anchor points H and C, moves during both heating and cooling. During a single heating up or cooling down process, the midpoint movement is half of point H, C, respectively ($\Delta u^{\mathrm{h}}_{\mathrm{mid}}=\Delta u_C/2$, $\Delta u^{\mathrm{c}}_{\mathrm{mid}}=\Delta u_H/2$). Considering H is static during heating and only moves during cooling (C is the opposite), the total movement of midpoint and virtual anchor points H and C for a whole 'heating + cooling' process is the same.

The movements of the pipeline ends, which have engineering importance for assessing the influence on end connected structures, are such that they always have a larger displacement along the direction of the activating force Q and relatively smaller displacements opposite to Q. These two incremental displacements (i.e. $\Delta u_{\mathrm{e}}^{Q+}$ the displacement along Q and $\Delta u_{\mathrm{e}}^{Q-}$ opposite to Q) are

$$\begin{cases}\dfrac{\Delta u_{\mathrm{e}}^{Q-}}{L}=-\dfrac{1-\eta}{2}\alpha\delta T+\mu\cos\theta\dfrac{W}{EA}\left(\dfrac{1-\eta}{2}\right)^2\\ \dfrac{\Delta u_{\mathrm{e}}^{Q+}}{L}=\dfrac{1+\eta}{2}\alpha\delta T-\mu\cos\theta\dfrac{W}{EA}\left(\dfrac{1-\eta}{2}\right)^2-\eta\alpha\delta T_{\mathrm{critical}}\end{cases} \tag{39}$$

The resultant displacements of the ends are $\Delta u_{\mathrm{e}}=\Delta u_{\mathrm{e}}^{Q+}+\Delta_{\mathrm{e}}^{Q-}$, and if the amplitudes of heating and cooling are the same $\delta T=\delta T_{\mathrm{h}}=\delta T_{\mathrm{c}}$, the end displacements are

$$\frac{\Delta u_{\mathrm{e}}}{L}=\frac{\Delta u_{\mathrm{e}}^{Q-}+\Delta u_{\mathrm{e}}^{Q+}}{L}=\alpha(\delta T-\delta T_{\mathrm{critical}})\eta \tag{40}$$

For a full heating up and cooling down cycle, the net displacement increments of virtual anchor points H, C, the midpoint and pipe ends – and in fact any point along the pipeline – are all the same. By assuming $\delta T=\delta T_{\mathrm{h}}=\delta T_{\mathrm{c}}$ for simplicity, the net walking distance per cycle, defined as the global incremental walking rate $\Delta u_{\mathrm{walking}}$ is

$$\frac{\Delta u_{\mathrm{walking}}}{L}=\alpha(\delta T-\delta T_{\mathrm{critical}})\eta \tag{41}$$

The term $\alpha(\delta T-\delta T_{\mathrm{citical}})$ represents the strain change for temperature changes exceeding the critical mobilising temperature, $\delta T_{\mathrm{citical}}$. The ratio η, between activating force Q and soil resistance $\mu W\cos\theta$, is the essential factor that controls the rate of axial walking. If η is positive (Q is along the x-axis), the pipeline moves downhill, and if η is negative, the pipeline moves uphill. If η (or Q) is equal to 0, the pipeline will not produce global axial cumulative displacement, with the pipeline just expanding and contracting symmetrically around the middle point during the cycles.

The effect of coupling and comparison with Carr et al. *(2006)*

If only the seabed slope is considered, with resultant end forces $F=0$, the activating force becomes $Q=W\sin\theta$.

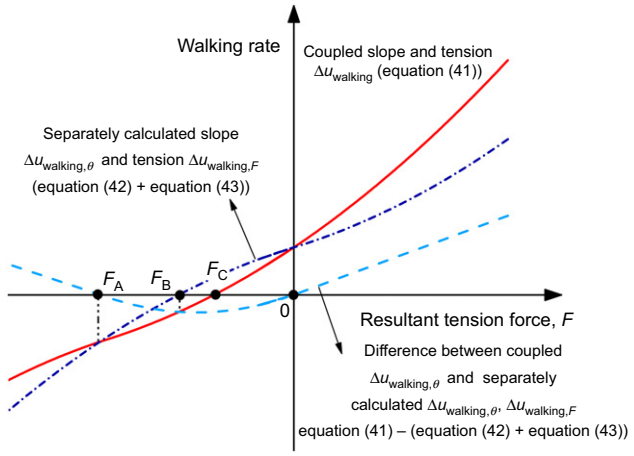

Fig. 7. The effect of coupling

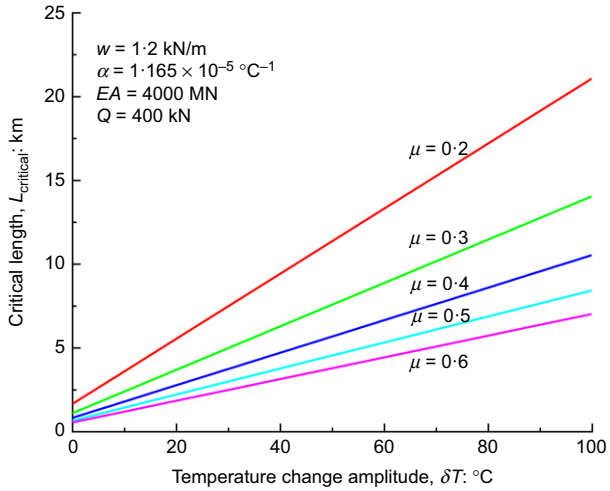

Fig. 8. Critical length

Similarly, if the pipeline is laid on a seabed with no slope, the activating force is the resultant tensile force $Q = F = F_b - F_t$. In these cases, equation (41) degrades respectively to

$$\frac{\Delta u_{\text{walking},\theta}}{L} = \left(\alpha\delta T - \frac{\mu W\cos\theta - |W\sin\theta|}{EA}\right)\frac{\tan\theta}{\mu} \tag{42}$$

$$\frac{\Delta u_{\text{walking},F}}{L} = \left(\alpha\delta T - \frac{\mu W - |F|}{EA}\right)\frac{F}{\mu W} \tag{43}$$

Equations (42) and (43) are exactly the same as the walking rate proposed by Carr *et al.* (2006), since their equations can be considered a special case of this study.

To demonstrate the effect of coupling, the walking rates calculated from equation (41) and the simple superposition of equation (42) and equation (43) are shown in Fig. 7. The walking rate $\Delta u_{\text{walking}}$ is under-predicted when coupling is not considered and superposition of the independent equations is used, for the case of a resultant tension force down the slope $F > 0$. The results are more complex for the reverse case of a tension force opposite to the direction of the seabed slope. Superposition overestimates the walking rate when $F_C < F < 0$. For $F_B < F < F_C$, superposition without coupling predicts downhill walking, while the coupled solution results in the pipeline walking uphill. Between F_A and F_B, superposition under-predicts the walking rate again (noting the negative rate implies walking uphill). However, when $F < F_A$ superposition predicts a larger magnitude (still negative) walking rate than the coupled solution. The values of F_A, F_B, F_C can be obtained by finding the roots of equation (41) − (equation (42) + equation (43)) = 0, as detailed in Appendix 2.

DISCUSSION ON WALKING CRITERION

Equivalence of pipeline length and temperature amplitude

Following Tørnes *et al.* (2000), pipelines can be divided into 'short' and 'long' pipelines, where 'short' pipelines have the susceptibility of axial walking and 'long' pipelines do not, because the soil resistance along a 'long' pipeline is sufficient to form a stationary segment confining the overall displacement. From the previous derivation, it can be seen that 'short' and 'long' pipelines are relatively related to the amplitude of the temperature change. If pipeline walking occurs, the pipeline needs to be fully activated to expand during heating and contract during cooling. The critical temperature $\delta T_{\text{critical}}$ (equation (33)) is the temperature required to mobilise axial walking, for a given pipeline length, L. Equivalently, equation (33) can be rewritten as an expression of a critical pipeline length, L_{critical}, if the temperature change magnitude δT is taken as input.

$$L_{\text{critical}} = \frac{\alpha EA\delta T + |Q|}{\mu w\cos\theta} \tag{44}$$

If the pipeline length is smaller than L_{critical}, it can be deemed a 'short' pipeline, where axial walking is prone to occur. Otherwise, if $L > L_{\text{critical}}$, it is a 'long' pipeline where no walking is possible. Carr *et al.* (2006) proposed a similar equation, where the term Q was not taken into account. Consequently, the equation of Carr *et al.* (2006) tends to underestimate the critical pipeline length. In other words, pipelines deemed as stable by Carr *et al.* (2006) can still present the possibility of exhibiting walking.

Figure 8 shows an estimation of the critical pipeline length by assuming a group of typical parameters, $w = 1{\cdot}2$ kN/m, $\alpha = 1{\cdot}165 \times 10^{-5}$°C^{-1}, $EA = 4000$ MN and $Q = 400$ kN, and with the seabed soil friction factor μ ranging from 0·2 to 0·6. For a temperature variation of 80°C, the critical pipeline length is 17·2, 11·5, 8·6, 6·9 and 5·7 km for μ ranging from 0·2 to 0·6.

Low temperature change

If a pipeline is long enough or if the temperature change is relatively small, the pipeline will be restrained by a stationary segment and thus no global pipeline walking will occur, although the pipeline ends still expand and contract. As shown in Fig. 4, when the pipeline heating temperature is small (or the pipeline is overly long), the middle segment [X_L, $L - X_R$] of the pipeline is constrained and shows zero displacement. Correspondingly, the axial displacement of the pipeline only happens near the ends of the pipeline (Fig. 4(d)). If the pipeline cools down from this state, the pipeline will gradually contract only around the segments close to the pipeline ends. In this case, the pipeline will not exhibit overall global axial walking.

Soil resistance evolution

The seabed soil resistance varies with the pipeline movement and loading history. Although the seabed soil may soften under cyclic loading, the more common case is that the seabed strength improves according to the degree of consolidation beneath the pipe (Hill *et al.*, 2012; White *et al.*, 2012). The relationships presented here need to reflect this, substituting an appropriate value of the friction

coefficient μ to reflect its evolution, generally increasing with time as a result of consolidation and the repeated cyclic movements. This will lead to a gradual reduction, potentially reducing to zero, of the walking rate. Further discussion on the evolution of soil strength under pipelines can be found in the outputs of the SAFEBUCK joint industry project (Bruton & Carr, 2011), such as in Bruton *et al.* (2006, 2009) and White *et al.* (2011, 2015).

CALCULATION EXAMPLES OF PIPELINE WALKING

This section demonstrates a group of calculation examples of pipeline walking based on the derived analytical solution. The calculation parameters are listed in Table 1. In many offshore fields, the transported content temperatures at the inlet of an offshore pipeline fall in the range 70–95°C (Harrison *et al.*, 2001; Anderson *et al.*, 2007; Jayson *et al.*, 2008). The temperature heating-up and cooling-down amplitude is considered to be equal to 100°C in this example, which is reasonable considering that it represents the equivalent in combined changes in both temperature and internal pressure. The tension values at the top and bottom of the pipeline are considered to be $F_t = 100$ kN and $F_b = 300$ kN and the seabed slope is $\theta = 2°$.

Table 1. Calculation parameters

Parameters	Value
Cross-sectional area of the pipeline, A	0·02 m^2
Pipeline length, L	5000 m
Pipe submerged weight, w	1200 N/m
Coefficient of friction, μ	0·5
Young's modulus, E	$2{\cdot}07 \times 10^{11}$ Pa
Poisson's ratio, v	0·3
Thermal expansion coefficient, α	$1{\cdot}165 \times 10^{-5}$ °C^{-1}

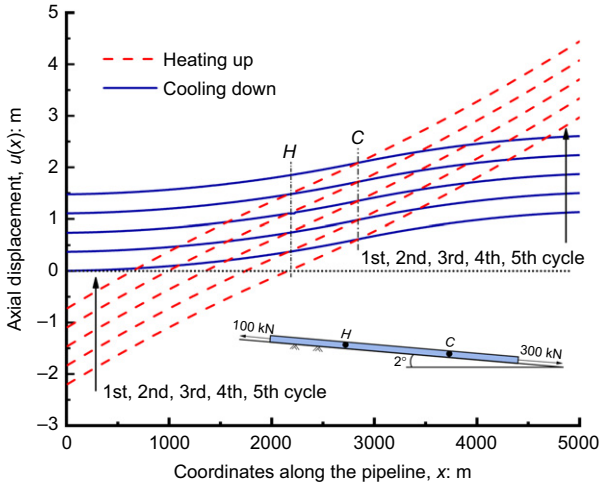

Fig. 9. Pipeline displacement profile

Cumulative displacement

The axial displacements for the first five cycles are shown in Fig. 9. The displacements for the two pipeline ends, the

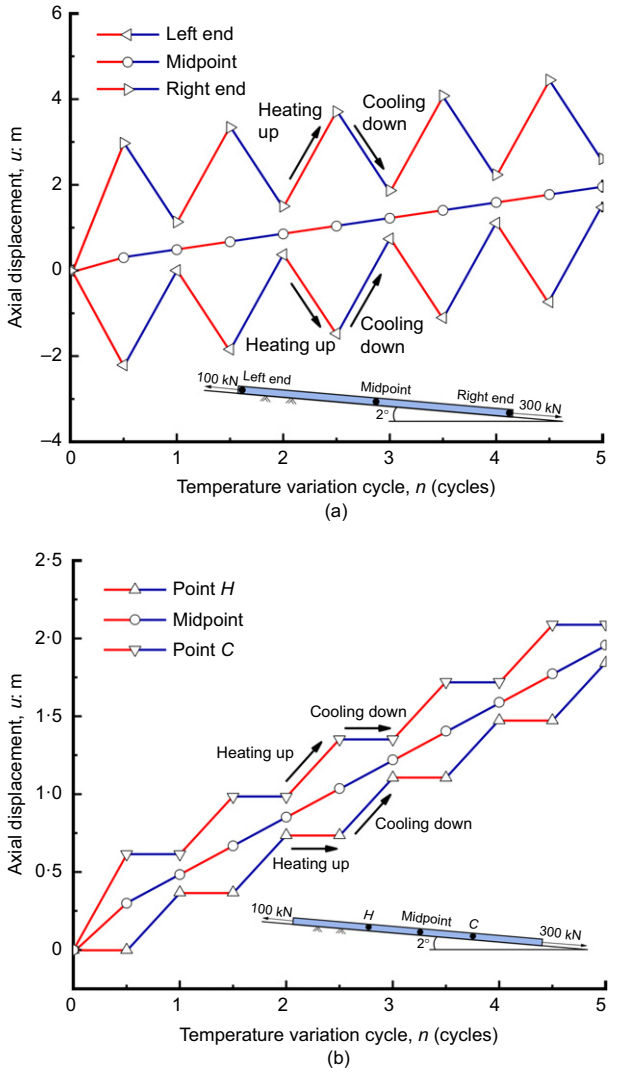

Fig. 10. Displacement history of the pipeline: (a) ends and midpoint; (b) point *H* and point *C*

Table 2. Calculated displacement (m)

Cycle number	State	Left end	Point *H*	Midpoint	Point *C*	Right end
0	Initial	0	0	0	0	0
1	Heating	−2·21	0·00	0·30	0·61	2·97
	Cooling	0·00	0·37	0·48	0·61	1·13
2	Heating	−1·84	0·37	0·67	0·98	3·34
	Cooling	0·37	0·74	0·85	0·98	1·50
3	Heating	−1·47	0·74	1·04	1·35	3·71
	Cooling	0·74	1·11	1·22	1·35	1·87
4	Heating	−1·10	1·11	1·41	1·72	4·08
	Cooling	1·14	1·47	1·59	1·72	2·24
5	Heating	−0·73	1·47	1·77	2·09	4·45
	Cooling	1·48	1·84	1·96	2·09	2·61

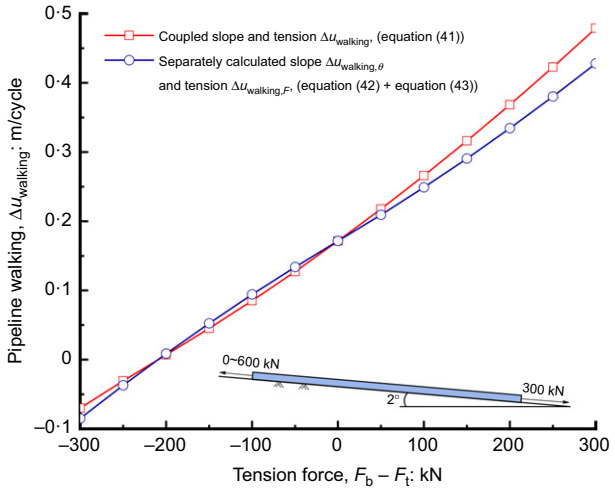

Fig. 11. The effect of coupling

virtual anchor points H and C and the midpoint are presented in Table 2 and are also shown in Fig. 10. When the pipeline heats up, the left end of the pipeline moves uphill and the right end of the pipeline moves downhill, indicating that the pipeline is expanding towards both ends. When the pipeline cools, the left end of the pipeline moves back and the right end of the pipe moves uphill, indicating that the pipeline is contracting inward. The activating force $Q = W\sin\theta + F_b - F_t = 409{\cdot}4$ kN from equation (8). Consequently, global pipeline walking occurs downhill along the seabed slope because of $Q > 0$. The two ends show greater downhill movement than uphill motion, where $\Delta u_e^{Q+} = 2{\cdot}21$ m and $\Delta u_e^{Q-} = -1{\cdot}84$ m from equation (39). In a complete heating and cooling cycle, the incremental displacement is $\Delta u_{walking} = 0{\cdot}37$ m.

The displacement of the pipeline midpoint is always downhill (positive) in the heating or cooling cycles. From equation (19), the displacement of the midpoint is 0·3 m during the first heating cycle and then exhibits a uniform displacement of 0·185 m during each individual heating and cooling cycle, as calculated from equation (38). In a complete heating and cooling cycle, the incremental displacement is 0·37 m. As can be seen in Fig. 10(b), the points H or C only displace during cooling or heating with a walking rate of 0·37 m/cycle.

Coupling effect

To demonstrate the coupling effect between slope and tension, the sensitivity to the resultant tension force $F = F_b - F_t$ was examined by varying it from −300 kN to 300 kN, while the seabed slope $\theta = 2°$ was kept unchanged. As shown in Fig. 11, the simple superposition of equations (42) and (43) can provide erroneous predictions of walking rate. When the tension force is large, the error can be significant. In this example, the error is 11% for a tension force of $F = 300$ kN.

CONCLUSIONS

Axial walking due to thermal changes or internal pressure fluctuations can cause damage to offshore pipelines and to their connected manifolds or steel catenary risers. This paper has established a complete analytical solution for pipeline walking that includes the coupling of the tensional force and the seabed slope while considering the pipe–soil sliding response to be rigid plastic. Equations to calculate the triggering of walking, the walking rate and the relationship between the critical length of the pipeline and the critical mobilising temperature are presented. The analytical solution, capable of considering any arbitrary heating and cooling amplitudes and the coupling between the two triggering mechanisms of tension and seabed slope, provides a rigorous and easy-to-use tool for pipeline walking analysis.

ACKNOWLEDGEMENTS

The authors acknowledge and appreciate discussions on pipeline walking that helped frame the ideas of this paper with Professor David White, now of the University of Southampton, during his time at the University of Western Australia's Centre for Offshore Foundation Systems. The second author appreciates Professor Chunhui Zhang from Hebei Science and Technology University and Dr Zhaohui Hong and Dr Dengfeng Fu from Tianjin University for their in-depth discussion and support (NSFC 51890913).

APPENDIX 1

$$\frac{u(x)}{L}=\begin{cases}\dfrac{(\mu\cos\theta-\sin\theta)W}{2EA}\left(\dfrac{x}{L}\right)^2+\left(\alpha\Delta T+\dfrac{F_t}{EA}\right)\dfrac{x}{L}-\dfrac{\sin\theta W}{EA}\left(\dfrac{X_S}{L}\right)^2-\dfrac{2Q}{EA}\dfrac{X_S}{L}\\ \quad+\left[\dfrac{(\mu\cos\theta+\sin\theta)W}{8EA}(1-\eta)-\dfrac{(\mu\cos\theta-\sin\theta)W}{2EA}\dfrac{X_S}{L}-\dfrac{1}{2}\left(\alpha\Delta T+\dfrac{F_t}{EA}\right)\right](1-\eta) & x\in[0,X_S]\\ \quad-\left[\alpha\Delta T+\left(\dfrac{F_b}{EA}-(\mu\cos\theta-\sin\theta)\right)\dfrac{W}{EA}\right]\eta+\dfrac{u_C}{L}\\ -\dfrac{(\mu\cos\theta+\sin\theta)W}{2EA}\left(\dfrac{x}{L}\right)^2+\left[\alpha\Delta T+\dfrac{(\mu\cos\theta-\sin\theta)W}{EA}\dfrac{X_S}{L}+\dfrac{F_t}{EA}\right]\dfrac{x}{L}-\dfrac{2Q}{EA}\dfrac{X_S}{L}\\ \quad+\left[\dfrac{(\mu\cos\theta+\sin\theta)W}{8EA}(1-\eta)-\dfrac{(\mu\cos\theta-\sin\theta)W}{2EA}\dfrac{X_S}{L}-\dfrac{1}{2}\left(\alpha\Delta T+\dfrac{F_t}{EA}\right)\right](1-\eta) & x\in[X_S,x_H]\\ \quad-\left[\alpha\Delta T+\left(\dfrac{F_b}{EA}-(\mu\cos\theta-\sin\theta)\right)\dfrac{W}{EA}\right]\eta+\dfrac{u_C}{L}\\ \dfrac{(\mu\cos\theta-\sin\theta)W}{2EA}\left(\dfrac{x}{L}\right)^2+\left\{\alpha\Delta T+\left[2\mu\cos\theta\dfrac{X_S}{L}+F_b-(\mu\cos\theta-\sin\theta)\right]\dfrac{W}{EA}\right\}\dfrac{x}{L}\\ \quad-\dfrac{(\mu\cos\theta-\sin\theta)W}{8EA}(1+\eta)^2 & x\in[x_H,L-X_S]\\ \quad-\dfrac{1}{2}\left\{\alpha\Delta T+\left[2\mu\cos\theta\dfrac{X_S}{L}+\dfrac{F_b}{EA}-(\mu\cos\theta-\sin\theta)\right]\dfrac{W}{EA}\right\}(1+\eta)+\dfrac{u_C}{L}\\ -\dfrac{(\mu\cos\theta+\sin\theta)W}{2EA}\left(\dfrac{x}{L}\right)^2+\left[\alpha\Delta T+\dfrac{(\mu\cos\theta+\sin\theta)W+F_b}{EA}\right]\dfrac{x}{L}\\ \quad-\dfrac{\mu W\cos\theta}{EA}\left(\dfrac{X_S}{L}\right)^2+\dfrac{2\mu W\cos\theta}{EA}\dfrac{X_S}{L}-\dfrac{(\mu\cos\theta-\sin\theta)W}{8EA}(1+\eta)^2\\ \quad+(1+\eta)\left[\dfrac{(\mu\cos\theta-\sin\theta)W}{2EA}-\dfrac{\mu\cos\theta W}{EA}\dfrac{X_S}{L}-\dfrac{1}{2}\left(\alpha\Delta T+\dfrac{F_b}{EA}\right)\right] & x\in[L-X_S,L]\\ \quad-\dfrac{\mu\cos\theta W}{EA}+\dfrac{u_C}{L}\end{cases}\tag{45}$$

where u_C is the displacement of point C (i.e. virtual anchor during cooling) accumulated in the previous cycles.

APPENDIX 2

As shown in Fig. 7, F_A can be calculated as the root of equation (41) − equation (42) + equation (43) = 0, as

$$F_A=-\frac{W\sin\theta}{2(1-\cos\theta)}+\frac{\alpha\delta TEA}{2}-\sqrt{\left[\frac{W\sin\theta}{2(1-\cos\theta)}-\frac{\alpha\delta TEA}{2}\right]^2-\frac{2W^2\sin^2\theta}{(1-\cos\theta)}}\tag{46}$$

F_B means the tension force when the simple superposition of walking rate from equations (42) and (43) is 0, as

$$F_B=(\alpha\delta TEA-\mu W)-\sqrt{(\alpha\delta TEA-\mu W)^2+4W\tan\theta(\alpha\delta TEA-\mu W\cos\theta+W\sin\theta)}\tag{47}$$

F_C means the tension force when the walking rate calculated from equation (41) is 0, which obviously is $F_C=-W\sin\theta$ – in other words, $Q=0$ and no walking occurs.

NOTATION

A pipeline cross-sectional area
C virtual anchor point during cooling down
D pipeline outer diameter
E Young's modulus of the pipeline material
F resultant tension force
$F_{A,B,C}$ value of the resultant tension with zero walking rate
F_b tension force applied at the bottom end of the pipeline
F_t tension force applied at the top end of the pipeline
f_0 soil resistance in the previous step
$f(x)$ soil resistance along the pipeline
H virtual anchor point during heating up
L total pipeline length
$L_{critical}$ critical pipeline length
$N(x)$ axial force along the pipeline
Q activating force
$T_{C,n}$ trough temperature in the nth cycle
$T_{H,n}$ peak temperature in the nth cycle
T_{ini} initial temperature of the pipeline
$u_{C,n}$ displacement of point C at the nth cycle
$u_{H,n}$ displacement of point H at the nth cycle

$u(x)$ axial displacement along the pipeline
u_S displacement of an arbitrarily selected point S
W total weight of pipeline
w pipeline weight per unit length
X_L length of the segment mobilised at the left end
X_R length of the segment mobilised at the right end
X_S length of the segment contracting during cooling
x coordinate along pipeline
x_C coordinate of stationary point C
x_H coordinate of stationary point H
x_{mid} coordinate of mid-point, $L/2$
α thermal expansion coefficient
ΔN_C axial force variation
$\Delta N_{C,mob}$ maximum axial force variation
Δp internal pressure
ΔT temperature variation relative to the initial temperature
$\Delta T_{h,mob}$ fully mobilised temperature during the first heating cycle
Δu incremental displacement
Δu_C incremental displacement of the point C
Δu_H incremental displacement of the point H
Δu_e^{Q+} incremental displacement of the pipe ends along the Q direction
Δu_e^{Q-} incremental displacement of the pipe ends opposite to the Q direction
$\Delta u_{mid}^{h,c}$ incremental displacement of the midpoint
$\Delta u_{walking}$ walking rate
$\Delta u_{walking,F}$ walking rate for the case of tensional force in the pipeline
$\Delta u_{walking,\theta}$ walking rate for the case of a sloped seabed
δT temperature change during heating or cooling
δT_c temperature change during cooling
$\delta T_{critical}$ fully mobilised temperature
δT_h temperature change during heating
$\varepsilon(x)$ axial strain along the pipeline
η ratio of activating force to soil resistance capacity
θ seabed slope
μ coefficient of friction
ν Poisson's ratio

REFERENCES

Anderson, M., Bruton, D. & Carr, M. (2007). The influence of pipeline insulation on installation temperature, effective force and pipeline buckling. In *ASME 2007 26th international conference on offshore mechanics and arctic engineering. Volume 3: pipeline and riser technology; CFD and VIV*, paper no. OMAE2007-29317, pp. 315–324. New York, NY, USA: American Society of Mechanical Engineers.

Bruton, D. & Carr, M. (2011). Overview of the SAFEBUCK JIP. *Proceedings of the offshore technology conference,* Houston, TX, USA, paper OTC 21671, https://doi.org/10.4043/21671-MS.

Bruton, D., White, D., Cheuk, C., Bolton, M. & Carr, M. (2006). Pipe/soil interaction behavior during lateral buckling, including large-amplitude cyclic displacement tests by the safebuck JIP. *Proceedings of the offshore technology conference,* Houston, TX, USA, paper OTC 17944, https://doi.org/10.4043/17944-MS.

Bruton, D., White, D., Carr, M. & Cheuk, C. (2008). Pipe-soil interaction during lateral buckling and pipeline walking – the SAFEBUCK JIP. *Proceedings of the offshore technology conference,* Houston, TX, USA, paper OTC 19589, https://doi.org/10.4043/19589-MS.

Bruton, D., White, D., Langford, T. & Hill, A. J. (2009). Techniques for the assessment of pipe-soil interaction forces for future deepwater developments. *Proceedings of the offshore technology conference,* Houston, TX, USA, paper OTC 20096, https://doi.org/10.4043/20096-MS.

Bruton, D., Sinclair, F. & Carr, M. (2010). Lessons learned from observing walking of pipelines with lateral buckles, including new driving mechanisms and updated analysis models. *Proceedings of the offshore technology conference,* Houston, TX, USA, paper OTC 20750, https://doi.org/10.4043/20750-MS.

Bruton, D., Carr, M. & MacRae, I. (2015). Pipe–soil friction or fiction. *Proceedings of the offshore pipeline technology conference*, Amsterdam, the Netherlands.

Carneiro, D., Gouveia, J., Parrilha, R., Oazen, E., Tardelli, L. & Cardoso, C. (2009). Design of small diameter HT/HP sour service reeled rigid pipelines. *Proceedings of the 7th Rio pipeline conference*, Rio de Janeiro, Brazil.

Carr, M., Bruton, D. & Leslie, D. (2003). Lateral buckling and pipeline walking, a challenge for hot pipelines. *Proceedings of the offshore pipeline technology conference*, Amsterdam, the Netherlands.

Carr, M., Sinclair, F. & Bruton, D. (2006). Pipeline walking – understanding the field layout challenges, and analytical solutions developed for the SAFEBUCK JIP. *Proceedings of the offshore technology conference,* Houston, TX, USA, paper OTC 17945, https://doi.org/10.4043/17945-MS.

Castelo, A., White, D. J. & Tian, Y. (2019). Simple solutions for downslope pipeline walking on elastic–perfectly-plastic soils. *Ocean Engng* **172**, 671–683.

Collberg, L., Carr, M. & Levold, E. (2011). Safebuck design guideline and DNV-RP-F110. *Proceedings of the offshore technology conference,* Houston, TX, USA, paper OTC 21575, https://doi.org/10.4043/21575-MS.

Draper, S., An, H., Cheng, L., White, D. J. & Griffiths, T. (2015). Stability of subsea pipelines during large storms. *Phil. Trans. R. Soc. A* **373**, No. 2033, 20140106.

Guha, I., White, D. J. & Randolph, M. F. (2019). Subsea pipeline walking with velocity dependent seabed friction. *Appl. Ocean Res.* **82**, 296–308.

Harrison, G. E., Harrison, M. S. & Bruton, D. (2001). King flowlines thermal expansion design and implementation. *Proceedings of the offshore technology conference,* Houston, TX, USA, paper OTC 15310, https://doi.org/10.4043/15310-MS.

Hill, A. J. & Jacob, H. (2008). *In situ* measurement of pipe–soil interaction in deep water. *Proceedings of the offshore technology conference,* Houston, TX, USA, paper OTC 19528, https://doi.org/10.4043/19528-MS.

Hill, A. J., White, D. J., Bruton, D., Langford, T., Meyer, V., Jewell, R. & Ballard, J. (2012). A new framework for axial pipe–soil resistance: illustrated by a range of marine clay datasets. In *Proceedings of the 8th international conference on offshore site investigation and geotechnics*, vol. 1, pp. 367–377. London, UK: Society for Underwater Technology.

Hobbs, R. E. (1984). In-service buckling of heated pipelines. *J. Transp. Engng* **110**, No. 2, 175–189.

Jayson, D., Delaporte, P., Albert, J. P., Prevost, M. E., Bruton, D. & Sinclair, F. (2008). Greater Plutonio project: subsea flowline design and performance. *Proceedings of the offshore pipeline technology conference*, London, UK.

Low, H., Ramm, M., Bransby, M. F., White, D. J. & Westgate, Z. (2017). Effect of through-life changes in soil strength and axial pipe–seabed resistance for HPHT pipeline design. *Proceedings of the 8th international conference on offshore site investigation and geotechnics*, pp. 841–849. London, UK: Society for Underwater Technology.

Palmer, A. C. & Baldry, J. A. S. (1974). Lateral buckling of axially constrained pipelines. *J. Petrol. Technol.* **26**, No. 11, 1283–1284.

Randolph, M. F. & Gourvenec, S. (2011). *Offshore geotechnical engineering*. Boca Raton, FL, USA: CRC Press.

Reda, A. M., Sultan, I. A., Howard, I. M., Forbes, G. L. & McKee, K. K. (2018). Pipeline walking and anchoring considerations in the presence of riser motion and inclined seabed. *Int. J. Press. Vessels Piping* **162**, 71–85.

Rong, H., Inglis, R., Bell, G., Huang, Z. & Chan, R. (2009). Evaluation and mitigation of axial walking with a focus on deep water flowlines. *Proceedings of the offshore technology conference,* Houston, TX, USA, paper OTC 19862.

Tian, Y. & Cassidy, M. (2008). Modelling of pipe–soil interaction and its application in numerical simulation. *Int. J. Geomech.* **8**, No. 4, 213–229.

Tian, Y., Cassidy, M. & Chang, C. (2015a). Assessment of offshore pipelines using dynamic lateral stability analysis. *Appl. Ocean Res.* **50**, 47–57.

Tian, Y., Youssef, B. & Cassidy, M. (2015b). Assessment of pipeline stability in the Gulf of Mexico during hurricanes using dynamic analysis. *Theor. Appl. Mech. Lett.* **5**, No. 2, 74–79.

Tørnes, K., Jury, J., Ose, B. & Thompson, P. (2000). Axial creeping of high temperature flowlines caused by soil ratcheting. *Proceedings of the ETCE/OMAE 2000 joint conference: energy*

for the new millennium, New Orleans, USA, vol. 2, pp. 1229–1239.

Tørnes, K., Zeitoun, H., Cumming, G. & Willcocks, J. (2009). A stability design rationale: a review of present design approaches. In *Proceedings of the 28th international conference on ocean, offshore and Arctic engineering*, pp. 717–729. New York, NY, USA: American Society of Mechanical Engineers.

White, D. J., Ganesan, S. A., Bolton, M. D., Bruton, D. A. S., Ballard, J. C. & Langford, T. (2011). SAFEBUCK JIP: observations from model testing of axial pipe–soil interaction on soft natural clays. *Proceedings of the offshore technology conference,* Houston, TX, USA, paper OTC 21249, https://doi.org/10.4043/21249-MS.

White, D. J., Campbell, M., Boylan, N. & Bransby, M. F. (2012). A new framework for axial pipe–soil resistance: illustrated by shearbox tests on carbonate soils. *Proceedings of the 8th international conference on offshore site investigation and geotechnics*, London, UK.

White, D. J., Westgate, Z. J., Ballard, J. C., de Brier, C. & Bransby, M. F. (2015). Best practice geotechnical characterization and pipe–soil interaction analysis for HPHT pipeline design. *Proceedings of the offshore technology conference,* Houston, TX, USA, paper OTC 26026, https://doi.org/10.4043/26026-MS.

Yu, H. T. & Yuan, Y. (2014). Analytical solution for an infinite Euler–Bernoulli beam on a viscoelastic foundation subjected to arbitrary dynamic loads. *J. Engng Mech.* **140**, No. 3, 542–551.

Yu, H. T., Cai, C., Yuan, Y. & Jia, M. C. (2017). Analytical solutions for Euler–Bernoulli beam on Pasternak foundation subjected to arbitrary dynamic loads. *Int. J. Numer. Analyt. Methods Geomech.* **41**, No. 8, 1125–1137.

Yu, H. T., Yang, Y. S. & Yuan, Y. (2018). Analytical solution for a finite Euler–Bernoulli beam with single discontinuity in section under arbitrary dynamic loads. *Appl. Math. Model.* **60**, 571–580.

Zeitoun, H. O., Tørnes, K., Li, J., Wong, S., Brevet, R. & Willcocks, J. (2009). Advanced dynamic stability analysis. In *Proceedings of the 28th international conference on ocean, offshore and Arctic engineering*, pp. 661–673. New York, NY, USA: American Society of Mechanical Engineers.

Zhou, T., Tian, Y., White, D. J. & Cassidy, M. J. (2019). Finite-element modeling of offshore pipeline lateral buckling. *J. Pipeline Syst. Engng Pract.* **10**, No. 4, 04019029.